PROCEEDINGS OF SCIENCE

Calibration of the integrating sphere for O4 in KAGRA gravitational wave telescope.

Shingo Fujii[a,*] **on behalf of the KAGRA collaboration**

[a] *Institute for Cosmic Ray Research, KAGRA Observatory, The University of Tokyo, 238 Higashi-Mozumi, Kamioka-cho, Hida City, Gifu 506-1205, Japan*

E-mail: shingo@icrr.tokyo.ac.jp

KAGRA, the gravitational wave telescope located in Japan, has started the 4th international observing run called O4 with LIGO and Virgo. The accuracy of parameter estimation for gravitational wave source objects depends on the accuracy of calibration. LIGO, Virgo, and KAGRA use the same calibration method called the photon calibrator (Pcal) method. In the Pcal system, we will obtain the precise displacement of a mirror induced by a well-calibrated radiation pressure of a laser beam which is injected into the mirror. As the uncertainty of the Pcal system is primarily limited by the uncertainty of the laser power measurement, we use integrating sphere (IS) power meters, which are considered to have good accuracy and precision, for the laser power measurement. However, during our calibration measurements in O3GK, we found that there were unidentified systematic errors in the laser power measurement. Therefore, we investigated the incident direction dependence and polarization dependence of the IS power meter.

According to our study, the angular dependence differs between two types of ISs, namely GPS (General Purpose Spheres) and LPM (Laser Power Measurement Spheres), which are utilized in our calibration system. The angular dependence of the GPS type was greater than that of the LPM type. The GPS measurement showed an approximate 8.4% increase from the value obtained with perpendicular incidence at maximum. In contrast, the LPM measurement showed a 0.2% increase from the value obtained with perpendicular incidence at maximum. As to polarization dependence, the effect of that on the LPM type was within the range of -0.06% to 0.06%. From this study, we found a possibility that the angle dependence was able to explain the uncertainty observed in O3GK.

In this proceeding, we report the angular and polarization dependence of ISs and consider the effect on the uncertainty of the KAGRA Pcal system.

38th International Cosmic Ray Conference (ICRC2023)
26 July - 3 August, 2023
Nagoya, Japan

*Speaker

PoS(ICRC2023)1553

1. Introduction

KAGRA, the gravitational wave telescope located in Japan, has started the 4th international observing run called O4 with LIGO and Virgo. About 90 gravitational wave events have been reported from previous LIGO and Virgo observations until O3 [1]. Enhanced sensitivity of gravitational wave telescopes is expected to increase the number of gravitational wave detections and the signal-to-noise ratio of each event. As signal-to-noise ratios increase, reduction of calibration uncertainty becomes more crucial in enhancing the accuracy and precision in parameter estimation for each gravitational wave source.

Calibration groups utilize the photon calibrator (Pcal) method to calibrate the gravitational wave signals and have been conducting to reduce its uncertainty [2]. In the Pcal method, laser beams are injected into a mirror of the interferometer and actuate the mirror with its radiation pressure. Consequently, these laser beams generate calibrated reference signals in the sensitivity curve of a GW detector. The reference signal is expressed as the displacement of the mirror, given by [3]

$$x(\omega) = -\frac{2P\cos\theta}{Mc\omega^2}, \tag{1}$$

where P is the Pcal laser power on the mirror surface, θ is incident angle of the laser beam on the mirror surface, M is the mass of mirrors, c is the speed of light. The uncertainty of the displacement is determined by the uncertainties of each parameter of the right side on Eq. 1. Currently, the uncertainty of the laser power is the most dominant component compared to other parameters. Accurate laser power measurements are essential to enhance accuracy and precision. To enhance accuracy and precision, we use integrating sphere (IS) power meters. The inner wall of the IS is constructed from materials with a reflectivity of over 96 % at the Pcal laser wavelength, 1047 nm [4], and this material exhibits properties of a perfect diffusion surface. These characteristics ensure an accurate and precise laser power measurement which is insensitive to variations in incident angle, polarization, and position of the laser beam. Owing to its high reflectivity and perfect diffusivity, the laser beam incident upon ISs undergoes multiple uniform reflections inside the sphere, resulting in a constant irradiance on the inner walls of ISs.

In the international observing run (O3GK) with GEO600, a 3% uncertainty was estimated to come from the IS calibration measurement [5]. This uncertainty could not be attributed to only statistical errors in measurements. Then, we decided to investigate the unknown systematic errors. We particularly focused on the characteristics of IS power meters, such as the incident angle dependence and polarization dependence of the injected laser.

2. Experimental setup

We use two types of ISs: 3P-040-LPM-SL (LPM) and 3P-GPS-060-SL (GPS) provided by Labsphere. These two types of the ISs differ in the relative position of the laser input port and the photodetector port, the presence of a baffle, and the size of the spheres and their port. The size of the GPS type is 6 inches, and that of the LPM type is 4 inches. Moreover, in the GPS type, a baffle is situated between the laser input port and the port for a photodetector to avoid direct

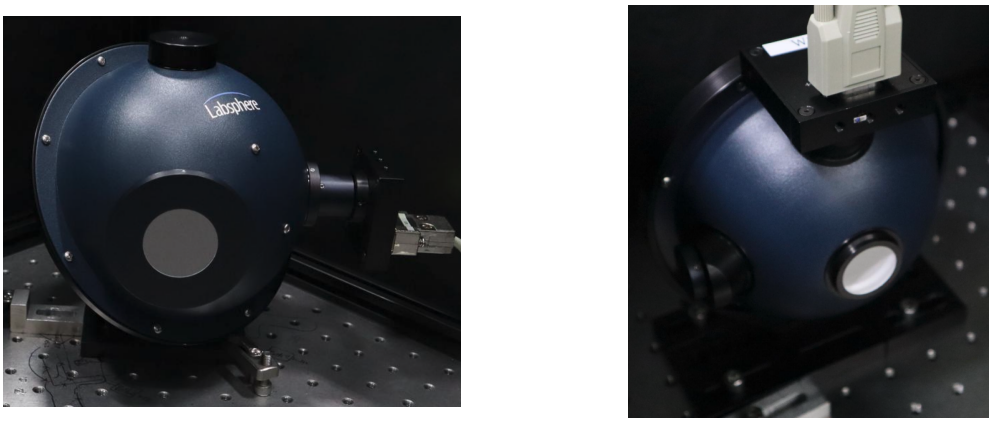

(a) GPS type

(b) LPM type

Figure 1: Two types of IS power meters. The photodetector is located on the right side of the figure for the GPS type and on the top side of the figure for the LPM type. The GPS type has a baffle between the laser input port and the port for a photodetector. The size of the GPS type is 6 inches, and that of the LPM type is 4 inches.

laser incidence, whereas, no baffle is in the LPM type. The above differences potentially create asymmetrical characteristics in the outputs of the ISs.

Figure 2 shows the schematic diagram of the experimental setup. We injected a laser with a wavelength of 1047 nm into two ISs and measure the voltage outputs of an IS power meter at position 1, V_1, and the voltage outputs at position 2, V_2. To mitigate the influence of incident laser power fluctuations, we took the ratio, V_1/V_2, and used this value as an evaluation index. Additionally, we used an Optical Follower Servo (OFS) system for the laser intensity stabilization for more reduction of the influence of the laser power fluctuations. In OFS, the intensity fluctuation was sampled at the OFS photodetector and it was feedback to the Acoustic Optical Modulator (AOM) to stabilize the main beam intensity fluctuation.

3. Angular dependence

The IS may have angular dependence due to, for example, the properties of their internal material and an asymmetrically located baffle inside. Actually, according to the data [6], the power per unit area of lasers reflected by the material varies depending on the direction of the reflection. Therefore, irradiance in the inner wall may vary depending on the position of the spheres, and its distribution also potentially differs in the incident angle of a laser beam. And, if a baffle is placed in an asymmetric position, the baffle has the potential to interrupt the generation of a uniform irradiance.

In order to measure the angular dependence of the ISs, we rotated the ISs at position 1 and calculated the ratio, V_1/V_2, where V_2 was the output voltage from the IS power meter at position 2, which monitored the laser power fluctuation. Figure 3 shows definitions of the center and directions of rotation. We defined 0 degrees as an incidence perpendicular to the IS, clockwise rotation to the laser beam as positive, and counterclockwise rotation as negative.

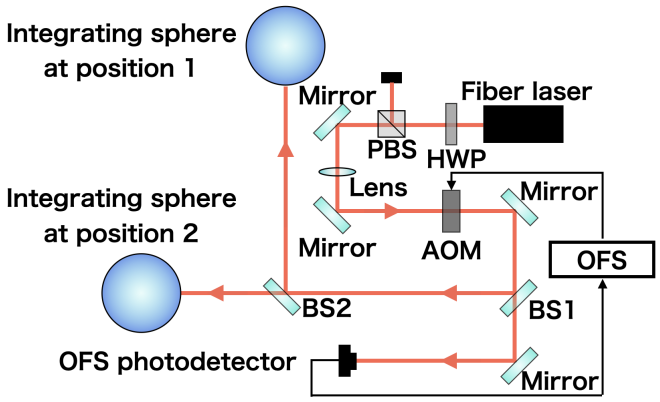

Figure 2: The schematic diagram of the experimental setup. An Optical Follower Servo (OFS) is used for laser intensity stabilization. We use an Acousto-Optic Modulator (AOM) as the laser beam power adjuster and the OFS photodetector to sample a portion of the laser beam power. The laser beam is divided at a Beam Splitter 2 (BS2). An IS power meter at position 2 is used as a reference for laser power fluctuations and the other IS at position 1 is used to measure its properties

In the LPM type measurement, we took data at one-degree intervals from -15 degrees to +15 degrees with 200 samples for each angle. On the other hand, in the GPS type measurement, we took data at one-degree intervals ranging from -15 degrees to +15 degrees with 400 samples taken for each angle. The reason why the data number of 400 for the GPS type is more than 200 for the LPM type is to mitigate the statistical error which was enhanced by the larger fluctuation of the voltage ratio of $V1/V2$.

The measurement results are shown in Figure 4. The vertical axis represents

$$\left(\frac{V_1/V_2}{V_1^{(0)}/V_2^{(0)}} - 1\right) \times 100, \tag{2}$$

where $V_1^{(0)}$ is V_1 at 0-degrees measurement, $V_2^{(0)}$ is V_2 at 0-degrees measurement. The horizontal axis is the incident angle. The data for the GPS type clearly shows that the output increases at angles below -13 degrees and that it reaches approximately 8.4% compared to the 0-degree incidence. For the other ranges, in the measurement for the GPS type, the deviation shows a linear tendency from -0.2% to 0.3%, whereas, in the measurement for the LPM type, the deviation is between 0.0% to 0.2%. One of the possibilities for why the GPS type has larger dependence on the laser beam incident angle than that of the LPM type is because the photodetector position of the GPS type is in the same plane where we changed the incident angles of the laser beam.

In the case of the GPS type, the deviation becomes 8.4% at maximum, which is much bigger than what we obtained in O3GK, 3%. Because we do not have information regarding the setting position of an IS and the Pcal laser paths during O3GK, the precise incident angles to the IS cannot be cleared. So, it is difficult to discuss the detailed effect in O3GK. However, we estimated that there was at least a 15-degree angle between the two laser beams. If so, there is a possibility that the angle dependence was able to explain the uncertainty observed in O3GK. Toward calibration

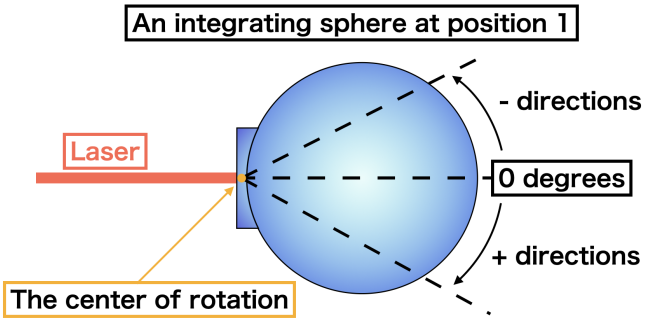

Figure 3: Incident angle definition. We define 0 degrees as the perpendicular incidence to the IS, clockwise rotation to the laser as positive, and counterclockwise rotation as negative.

measurements for O4, we are now controlling and recording the angle of incidence of the laser beam to the ISs to eliminate its influence.

4. Polarization dependence

The IS potentially exhibits polarization dependence due to, for example, the glass cover of the photodetector, which might have polarization dependence on the transmittance. If the light entering the photodetector retains residual polarization caused by an incomplete diffusion surface, the output will vary depending on the polarization state of the incident laser beam.

For the measurement of the polarization dependence, we developed a system to rotate the IS against an incident laser beam. The reason why we do not use a half-wave plate for rotating the linear polarization to the ISs is that we cannot distinguish the polarization dependence of the half-wave plate itself and the ISs.

Figure 5 shows the schematic diagram of the experimental setup for the polarization dependence measurement. A right angle kinematic mirror mount was used to redirect the laser's optical axis perpendicular to the optical table. We positioned the ISs to ensure that the laser beam was injected vertically and passed through the center of the rotation. The center of rotation for the IS is set at the center of the laser input port. The measurement for the LPM type was conducted, while the measurement for the GPS type is the future work. The data was taken at 10-degree intervals from 0 to 230 degrees with 200 samples. The date from 230 to 360 degrees could not be done because of the cable route constrain.

Figure 6 shows the results. The vertical axis shows values obtained by substituting $\overline{V_1/V_2}$ for $V_1^{(0)}/V_2^{(0)}$ in Eq. 2, where $\overline{V_1/V_2}$ is the arithmetic average of V_1/V_2. The horizontal axis is the rotation angle. This result shows that the deviation remains within the range of -0.06% to 0.06%. By the way, because linear polarization has symmetry at every 180-degree rotation, one could expect the same results at every 180-degree interval. However, Figure 6 does not exhibit such periodic patterns. So, this variation could be related to other factors. From these results, we conclude that the effect of the polarization of the LPM is less than ±0.06%, which is much lesser than what we observed at O3GK, 3%.

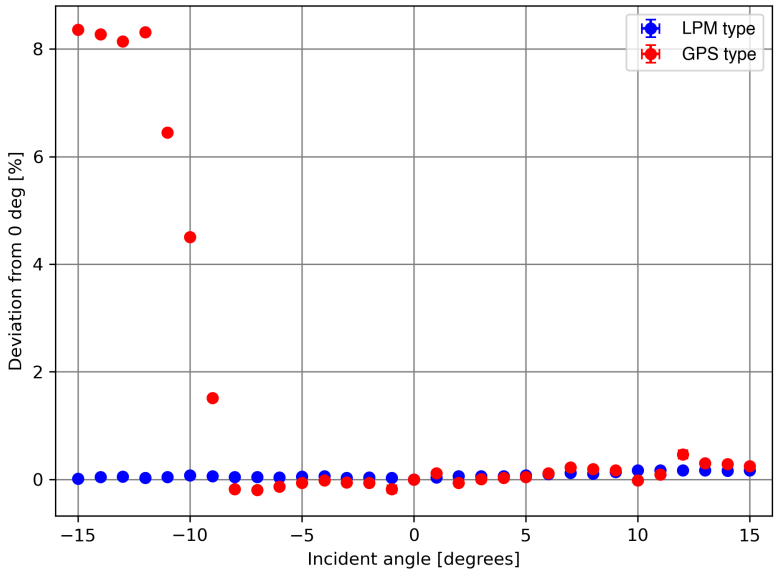

(a)

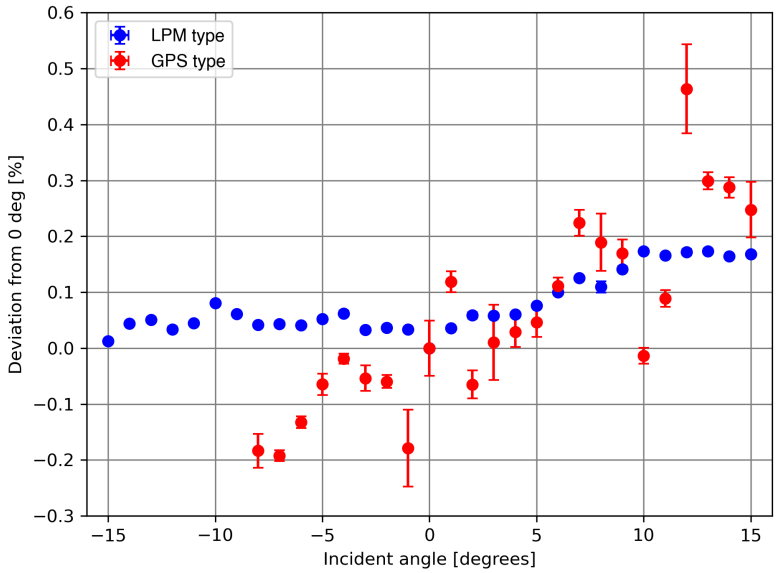

(b)

Figure 4: Result of angular dependence research. The vertical axis represents $\left(\frac{V_1/V_2}{V_1^{(0)}/V_2^{(0)}} - 1\right) \times 100$, where $V_1^{(0)}$ is V_1 at 0-degrees measurement, $V_2^{(0)}$ is V_2 at 0-degrees measurement. The horizontal axis represents the angle of incidence, while the vertical axis represents the difference from the 0-degree measurement expressed as a percentage. (a) represents the overall view, while (b) represents an enlarged view of figure (a) within the range of -0.2% to 0.5%. The error bars represent statistical errors.

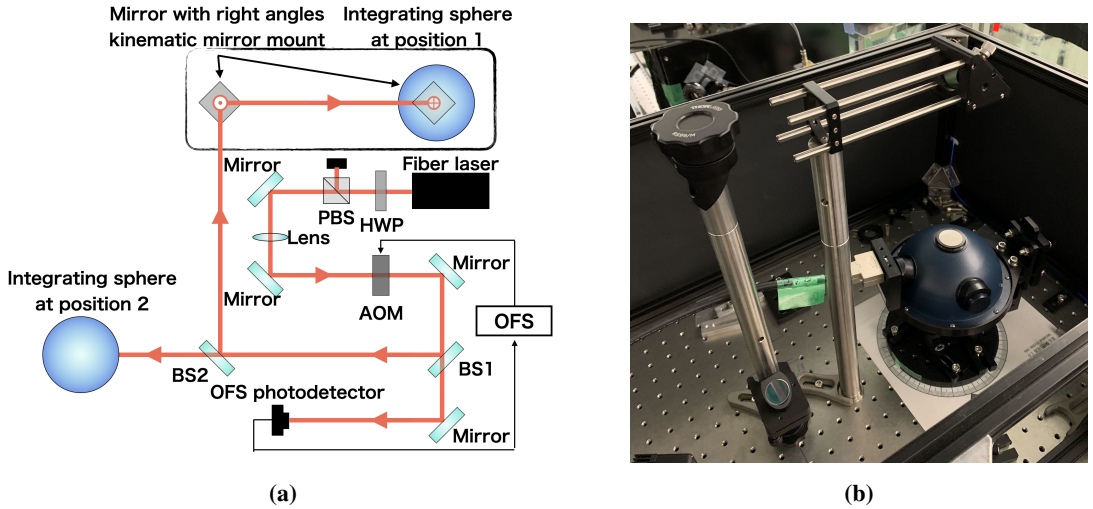

(a) **(b)**

Figure 5: (a) is an experimental setup for polarization dependence measurements. (b) is the photo image of the area enclosed in black line in (a).

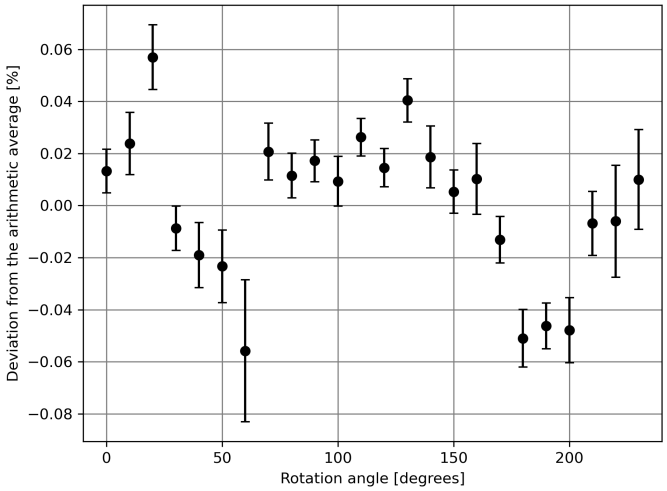

Figure 6: Result of polarization dependence of the LPM type. The vertical axis represents $\left(\frac{V_1/V_2}{\overline{V_1/V_2}} - 1\right) \times 100$, where $\overline{V_1/V_2}$ is the arithmetic average of V_1/V_2. The horizontal axis is the rotation angle and the vertical axis is the difference from the arithmetic mean of the measured points expressed as a percentage. The error bars represent statistical errors.

5. Summary and Future Work

Based on the angular dependence experiment, the maximum deviation reached 8.4% which was significantly larger than the 3% observed in O3GK. As to polarization dependence, the effect of that on the LPM type was one order smaller than the 3% uncertainty. The effect of the polarization dependence is within the range of -0.06% to 0.06%.

We plan to measure the polarization dependence of the GPS type. And, we plan to assess whether the uncertainties in laser power measurements using ISs in O4 can be explained by the variations caused by angular and polarization dependence based on the results of these experiments.

References

[1] R Abbott, et al., GWTC-3: compact binary coalescences observed by LIGO and Virgo during the second part of the third observing run, arXiv preprint arXiv:2111.03606, (2021).

[2] S. Karki, et al., Toward Calibration of the Global Network of Gravitational Wave Detectors with Sub-Percent Absolute and Relative Accuracy, Galaxies 2022, 10(2), 42 (2022).

[3] E. Goetz et al., Precise calibration of LIGO test mass actuators using photon radiation pressure. Class, Quantum Grav., 26:245011, (2009).

[4] Labsphere advancing the technology of light, Integrating Sphere Theory and Applications, PB-16011-000 Rev.00, (2017).

[5] T. Akutsu, et al., Overview of KAGRA:Calibration, detector characterization, physical environmental monitors, and the geophysics interferometer, Prog. Theor. Exp. Phys, 2021, 05A102 (2021).

[6] Labsphere advancing the technology of light, Reflectance Coatings and Materials, PB-14117-000 Rev 03, (2023).

Full Authors List: KAGRA Collaboration

H. Abe[1], T. Akutsu[2,3], M. Ando[4,5], M. Aoumi[6], A. Araya[7], N. Aritomi[8], Y. Aso[2,9], S. Bae[10], R. Bajpai[2], K. Cannon[5], Z. Cao[11], R.-J. Chang[12], A. H.-Y. Chen[13], D. Chen[14], H. Chen[15], Y. Chen[15], A. Chiba[16], R. Chiba[17], C. Chou[18], M. Eisenmann[2], S. Fujii[6], I. Fukunaga[19], D. Haba[1], S. Haino[20], W.-B. Han[21], H. Hayakawa[6], K. Hayama[22], Y. Himemoto[23], N. Hirata[2], C. Hirose[24], S. Hoshino[24], H.-F. Hsieh[25], C. Hsiung[26], S.-C. Hsu[27,25], D. C. Y. Hui[28], K. Inayoshi[29], Y. Itoh[19,30], M. Iwaya[17], H.-B. Jin[31,32], K. Jung[33], T. Kajita[34], M. Kamiizumi[6], N. Kanda[30,19], J. Kato[16], T. Kato[17], S. Kim[28], N. Kimura[6], T. Kiyota[19], K. Kohri[35], K. Kokeyama[36], K. Komori[5,4], A. K. H. Kong[25], N. Koyama[24], J. Kume[5], S. Kuroyanagi[38,37], S. Kuwahara[5], K. Kwak[33], S. Lai[18], H. W. Lee[39], R. Lee[15], S. Lee[40], M. Leonardi[41,2], K. L. Li[12], L. C.-C. Lin[12], C-Y. Lin[42], E. T. Lin[25], G. C. Liu[26], L.-T. Ma[25], K. Maeda[16], M. Matsuyama[19], M. Meyer-Conde[19], Y. Michimura[43,5], N. Mio[44], O. Miyakawa[6], S. Miyamoto[17], S. Miyoki[6], S. Morisaki[17], Y. Moriwaki[16], M. Murakoshi[45], K. Nakamura[2], H. Nakano[46], T. Narikawa[17], L. Nguyen Quynh[47], Y. Nishino[2,48], A. Nishizawa[5], K. Obayashi[45], J. J. Oh[49], K. Oh[28], M. Ohashi[6], M. Ohkawa[24], K. Oohara[50,51], Y. Oshima[4], S. Oshino[6], M. A. Page[2], K.-C. Pan[15,25], J. Park[40], F. E. Peña Arellano[6], S. Saha[25], K. Sakai[52], T. Sako[16], R. Sato[24], S. Sato[16], Y. Sato[16], T. Sawada[6], Y. Sekiguchi[53], L. Shao[29], Y. Shikano[54,55], K. Shimode[6], H. Shinkai[56], J. Shiota[45], K. Somiya[1], T. Suzuki[24], T. Suzuki[1], H. Tagoshi[17], H. Takahashi[57], R. Takahashi[2], A. Takamori[7], K. Takatani[19], H. Takeda[58], M. Takeda[19], M. Tamaki[17], K. Tanaka[59], S. J. Tanaka[45], T. Tanaka[58], A. Taruya[60], T. Tomaru[2], K. Tomita[19], T. Tomura[6], A. Toriyama[45], A. A. Trani[5], S. Tsuchida[61], N. Uchikata[17], T. Uchiyama[6], T. Uehara[62], K. Ueno[5], T. Ushiba[6], M. H. P. M. van Putten[63], H. Wang[4], T. Washimi[2], C. Wu[15], H. Wu[15], K. Yamamoto[16], M. Yamamoto[16], T. Yamamoto[6], T. S. Yamamoto[37], S. Yamamura[17], R. Yamazaki[45], L.-C. Yang[18], Y. Yang[18], S.-W. Yeh[15], J. Yokoyama[5,4], T. Yokozawa[6], H. Yuzurihara[6], Y. Zhao[17,2], Z.-H. Zhu[11,64]

[1]Graduate School of Science, Tokyo Institute of Technology, 2-12-1 Ookayama, Meguro-ku, Tokyo 152-8551, Japan. [2]Gravitational Wave Science Project, National Astronomical Observatory of Japan, 2-21-1 Osawa, Mitaka City, Tokyo 181-8588, Japan. [3]Advanced Technology Center, National Astronomical Observatory of Japan, 2-21-1 Osawa, Mitaka City, Tokyo 181-8588, Japan. [4]Department of Physics, The University of Tokyo, 7-3-1 Hongo, Bunkyo-ku, Tokyo 113-0033, Japan. [5]Research Center for the Early Universe (RESCEU), The University of Tokyo, 7-3-1 Hongo, Bunkyo-ku, Tokyo 113-0033, Japan. [6]Institute for Cosmic Ray Research, KAGRA Observatory, The University of Tokyo, 238 Higashi-Mozumi, Kamioka-cho, Hida City, Gifu 506-1205, Japan. [7]Earthquake Research Institute, The University of Tokyo, 1-1-1 Yayoi, Bunkyo-ku, Tokyo 113-0032, Japan. [8]LIGO Hanford Observatory, Richland, WA 99352, USA. [9]The Graduate University for Advanced Studies (SOKENDAI), 2-21-1 Osawa, Mitaka City, Tokyo 181-8588, Japan. [10]Korea Institute of Science and Technology Information (KISTI), 245 Daehak-ro, Yuseong-gu, Daejeon 34141, Republic of Korea. [11]Department of Astronomy, Beijing Normal University, Xinjiekouwai Street 19, Haidian District, Beijing 100875, China. [12]Department of Physics, National Cheng Kung University, No.1, University Road, Tainan City 701, Taiwan. [13]Institute of Physics, National Yang Ming Chiao Tung University, 101 Univ. Street, Hsinchu, Taiwan. [14]Kamioka Branch, National Astronomical Observatory of Japan, 238 Higashi-Mozumi, Kamioka-cho, Hida City, Gifu 506-1205, Japan. [15]Department of Physics, National Tsing Hua University, No. 101 Section 2, Kuang-Fu Road, Hsinchu 30013, Taiwan. [16]Faculty of Science, University of Toyama, 3190 Gofuku, Toyama City, Toyama 930-8555, Japan. [17]Institute for Cosmic Ray Research, KAGRA Observatory, The University of Tokyo, 5-1-5 Kashiwa-no-Ha, Kashiwa City, Chiba 277-8582, Japan. [18]Department of Electrophysics, National Yang Ming Chiao Tung University, 101 Univ. Street, Hsinchu, Taiwan. [19]Department of Physics, Graduate School of Science, Osaka Metropolitan University, 3-3-138 Sugimoto-cho, Sumiyoshi-ku, Osaka City, Osaka 558-8585, Japan. [20]Institute of Physics, Academia Sinica, 128 Sec. 2, Academia Rd., Nankang, Taipei 11529, Taiwan. [21]Shanghai Astronomical Observatory, Chinese Academy of Sciences, 80 Nandan Road, Shanghai 200030, China. [22]Department of Applied Physics, Fukuoka University, 8-19-1 Nanakuma, Jonan, Fukuoka City, Fukuoka 814-0180, Japan. [23]College of Industrial Technology, Nihon University, 1-2-1 Izumi, Narashino City, Chiba 275-8575, Japan. [24]Faculty of Engineering, Niigata University, 8050 Ikarashi-2-no-cho, Nishi-ku, Niigata City, Niigata 950-2181, Japan. [25]Institute of Astronomy, National Tsing Hua University, No. 101 Section 2, Kuang-Fu Road, Hsinchu 30013, Taiwan. [26]Department of Physics, Tamkang University, No. 151, Yingzhuan Rd., Danshui Dist., New Taipei City 25137, Taiwan. [27]Department of Physics, University of Washington, 3910 15th Ave NE, Seattle, WA 98195, USA. [28]Department of Astronomy and Space Science, Chungnam National University, 9 Daehak-ro, Yuseong-gu, Daejeon 34134, Republic of Korea. [29]Kavli Institute for Astronomy and Astrophysics, Peking University, Yiheyuan Road 5, Haidian District, Beijing 100871, China. [30]Nambu Yoichiro Institute of Theoretical and Experimental Physics (NITEP), Osaka Metropolitan University, 3-3-138 Sugimoto-cho, Sumiyoshi-ku, Osaka City, Osaka 558-8585, Japan. [31]National Astronomical Observatories, Chinese Academic of Sciences, 20A Datun Road, Chaoyang District, Beijing, China. [32]School of Astronomy and Space Science, University of Chinese Academy of Sciences, 20A Datun Road, Chaoyang District, Beijing, China. [33]Department of Physics, Ulsan National Institute of Science and Technology (UNIST), 50 UNIST-gil, Ulju-gun, Ulsan 44919, Republic of Korea. [34]Institute for Cosmic Ray Research, The University of Tokyo, 5-1-5 Kashiwa-no-Ha, Kashiwa City, Chiba 277-8582, Japan. [35]Institute of Particle and Nuclear Studies (IPNS), High Energy Accelerator Research Organization (KEK), 1-1 Oho, Tsukuba City, Ibaraki 305-0801, Japan. [36]School of Physics and Astronomy, Cardiff University, The Parade, Cardiff, CF24 3AA, UK. [37]Department of Physics, Nagoya University, ES building, Furocho, Chikusa-ku, Nagoya, Aichi 464-8602, Japan. [38]Instituto de Fisica Teorica UAM-CSIC, Universidad Autonoma de Madrid, 28049 Madrid, Spain. [39]Department of Computer Simulation, Inje University, 197 Inje-ro, Gimhae, Gyeongsangnam-do 50834, Republic of Korea. [40]Technology Center for Astronomy and Space Science, Korea Astronomy and Space Science Institute (KASI), 776 Daedeokdae-ro, Yuseong-gu, Daejeon 34055, Republic of Korea. [41]Department of Physics, University of Trento, via Sommarive 14, Povo, 38123 TN, Italy. [42]National Center for High-performance computing, National Applied Research Laboratories, No. 7, R&D 6th Rd., Hsinchu Science Park, Hsinchu City 30076, Taiwan. [43]LIGO Laboratory , California Institute of Technology, 1200 East California Boulevard, Pasadena, CA 91125, USA. [44]Institute for Photon Science and Technology, The University of Tokyo,

2-11-16 Yayoi, Bunkyo-ku, Tokyo 113-8656, Japan. [45]Department of Physical Sciences, Aoyama Gakuin University, 5-10-1 Fuchinobe, Sagamihara City, Kanagawa 252-5258, Japan. [46]Faculty of Law, Ryukoku University, 67 Fukakusa Tsukamoto-cho, Fushimi-ku, Kyoto City, Kyoto 612-8577, Japan. [47]Department of Physics and Astronomy, University of Notre Dame, 225 Nieuwland Science Hall, Notre Dame, IN 46556, USA. [48]Department of Astronomy, The University of Tokyo, 7-3-1 Hongo, Bunkyo-ku, Tokyo 113-0033, Japan. [49]National Institute for Mathematical Sciences, 70 Yuseong-daero, 1689 Beon-gil, Yuseong-gu, Daejeon 34047, Republic of Korea. [50]Graduate School of Science and Technology, Niigata University, 8050 Ikarashi-2-no-cho, Nishi-ku, Niigata City, Niigata 950-2181, Japan. [51]Niigata Study Center, The Open University of Japan, 754 Ichibancho, Asahimachi-dori, Chuo-ku, Niigata City, Niigata 951-8122, Japan. [52]Department of Electronic Control Engineering, National Institute of Technology, Nagaoka College, 888 Nishikatakai, Nagaoka City, Niigata 940-8532, Japan. [53]Faculty of Science, Toho University, 2-2-1 Miyama, Funabashi City, Chiba 274-8510, Japan. [54]Graduate School of Science and Technology, Gunma University, 4-2 Aramaki, Maebashi, Gunma 371-8510, Japan. [55]Institute for Quantum Studies, Chapman University, 1 University Dr., Orange, CA 92866, USA. [56]Faculty of Information Science and Technology, Osaka Institute of Technology, 1-79-1 Kitayama, Hirakata City, Osaka 573-0196, Japan. [57]Research Center for Space Science, Advanced Research Laboratories, Tokyo City University, 8-15-1 Todoroki, Setagaya, Tokyo 158-0082, Japan. [58]Department of Physics, Kyoto University, Kita-Shirakawa Oiwake-cho, Sakyou-ku, Kyoto City, Kyoto 606-8502, Japan. [59]Institute for Cosmic Ray Research, Research Center for Cosmic Neutrinos, The University of Tokyo, 5-1-5 Kashiwa-no-Ha, Kashiwa City, Chiba 277-8582, Japan. [60]Yukawa Institute for Theoretical Physics (YITP), Kyoto University, Kita-Shirakawa Oiwake-cho, Sakyou-ku, Kyoto City, Kyoto 606-8502, Japan. [61]National Institute of Technology, Fukui College, Geshi-cho, Sabae-shi, Fukui 916-8507, Japan. [62]Department of Communications Engineering, National Defense Academy of Japan, 1-10-20 Hashirimizu, Yokosuka City, Kanagawa 239-8686, Japan. [63]Department of Physics and Astronomy, Sejong University, 209 Neungdong-ro, Gwangjin-gu, Seoul 143-747, Republic of Korea. [64]School of Physics and Technology, Wuhan University, Bayi Road 299, Wuchang District, Wuhan, Hubei, 430072, China.

PoS(ICRC2023)1553